F.T. Smith

Combining Theory and Computations for Transition

Abstract

A combination of theory and computation seems needed, with physical understanding, to improve computational capabilities especially at high Reynolds numbers, where numerous paths occur in deep transition (the later stages of transition). This contribution shows recent developments. Certain aspects of the combination have been followed through mostly in 2D for the TS path alone: e.g. composite approaches followed by parabolized stability approaches. The theory is being extended into deep transition. A challenge is to obtain a theory-computation duet for 3D at large Reynolds numbers and capture most relevant paths. Parts of the 3D theory are in place and include encouraging agreements with experiments, on the first spike, on the Klebanoff and Nishioka paths, on transitional spot characteristics, on other transition paths; and the theory is now being developed further; but the repercussions for computations have still to be followed through.

Introduction (item 1)

To be specific we concentrate on spikes and nonlinear spots in transition, mostly for incompressible boundary layers. The emphasis is towards strong nonlinearity. Starting with spikes, the theory used herein is that of 2D or 3D interacting boundary layers (IBL), capturing nonlinear TS waves or following a vortex-wave interaction. Finite-time break-up produces shortened scales, yielding agreement with computations and experiments on the first spike in transition, with subsequent spot formation. After the break-up normal pressure gradients and vortex wind-up become significant locally. Also discussed herein are initial-value problems for spots containing a wide band of 3D nonlinear disturbances. The theory points to successive nonlinear stages starting at the wing tips near the spot trailing edge but gradually entering the middle as the amplitudes increase, downstream. This effect combined with shortening scales produces a spread angle near 11°, close to experimental observations. Viscosity enters later as for the spikes above originating near the surface or through a novel interaction influencing the global spot. This research on spikes, spots and their reproductions is directed towards greater understanding of deep transition. The theoretical understanding, e.g. of scales, should help Direct Numerical Simulations by determining which terms in the Navier-Stokes equations matter in any zone of flow and/or by interpreting results and/or by suggesting improved simulation methods, as well as providing parameterization and comparisons with experiments. Here, through addressing spikes and spots, we highlight three main nonlinear theories, vortex/wave interaction theory, pressure-displacement IBL theory, high-frequency cum Euler-scale theory, corresponding basically to increasing amplitudes. These nonlinear interactions can completely alter the mean-flow profiles. Their major assumption is that the global Reynolds number *Re* is large, in line with practical interest: eg. see comparisons herein at both subcritical and supercritical Re values.

First, item 2 below on *spikes*, e.g. in forced transition, considers nonlinear TS or IBL interactions, controlled by the unsteady IBL equations. Emphasis is given to nonlinear finite-time breakups, detailed comparisons with computations and experiments, and the repercussions. This breakup involves the scaled pressure gradient and skin friction becoming unbounded locally. A change of scales is therefore induced. The repercussions are concerned principally with sublayer eruption and vortex formation.

Second, numerous aspects of turbulent *spots* have been studied experimentally, e.g. the main arrowhead-shaped spot, its tail, its notional speed, and spreading rate. From reviews by Clark *et al.* (1994), Henningson *et al.* (1994), Seifert *et al.* (1994), Shaikh & Gaster (1994), Smith *et al.* (1994), much of the spot dynamics resembles that in a fully turbulent boundary layer; a spot develops fast from localized disturbances with large initial amplitude; growth and spreading perhaps take place in a domino-like manner, via successive production of hairpin vortices, or by other mechanisms; spanwise growth greatly exceeds normal growth; the leading edge and side edges are sharp, with side-interaction with trailing wave packets. Again computations have been performed; see reviews above. Much extra physical understanding has still to be provided, nevertheless. Systematic tracking of increasing amplitudes remains absent, experimentally and computationally. Few if any systematic theoretical studies had been made until recently. The research below appears the only effort towards strongly nonlinear theory, for spot evolutions as initial-value problems. Much of the experimental findings can be described by the theory, even though many complex phenomena arise during spot evolution. The Euler stage examined corresponds to disturbance wavenumbers α, β, frequencies ω, propagation speeds c and amplitudes (e.g. pressure p', velocity $\underline{u}'$) all of $0(1)$, based on the boundary-layer thickness and local freestream speed, thus representing a wider range than conventional linear-type TS disturbances which have $\alpha, \beta, \omega, c, |p'|, |\underline{u}'|$ all smaller. In consequence, it seems not unreasonable to proceed first by means of the Euler-stage approach, but as a nonlinear 3D initial-value problem for a localized input disturbance. This is the concern of much of item 3.

Item 3 splits the *spot* dynamics into global (mainly inviscid) and internal (viscous-inviscid) properties, and concentrates on the former. Nevertheless, a new long/short-scale global interaction is identified linking the 3D boundary-layer equations and unsteady Euler equations via Reynolds-stress forces, far downstream. Moreover, internal properties, flow structures and interactions with global dynamics are mentioned, having been addressed in item 2. The viscous sublayer, its eruptions and ensuing vortex formations can become important in practice. They introduce shorter length and time scales, and hence even higher frequency and wavenumber content, and they play a key part in the domino process. Item 3 is aimed at relatively high-amplitude nonlinear responses, as opposed to gradual transition. Further comments are in item 4.

IBL transitions and breakup: spikes (item 2)

The velocities $(\overline{u}, \overline{v}, \overline{w})$ in Cartesian coordinates $(\overline{x}, \overline{y}, \overline{z})$ (streamwise, normal, spanwise), pressure $\overline{p}$ and time $\overline{t}$ are nondimensionalized globally, with respect to (say) airfoil chord and freestream speed, and then scaled. So, near the typical 0(1) station $\overline{x} = \overline{x}_0$, $\overline{z} = \overline{z}_0$, the sublayer flow problem reduces to the unsteady nonlinear IBL one:

$$\frac{\partial \bar{u}}{\partial \bar{x}} + \frac{\partial \bar{v}}{\partial \bar{y}} + \frac{\partial \bar{w}}{\partial \bar{z}} = 0 \, , \tag{1}$$

$$\left(\frac{\partial}{\partial \bar{t}} + \bar{u}\frac{\partial}{\partial \bar{x}} + \bar{v}\frac{\partial}{\partial \bar{y}} + \bar{w}\frac{\partial}{\partial \bar{z}}\right)(\bar{u}, \bar{w}) = -\left(\frac{\partial \bar{p}}{\partial \bar{x}}, \frac{\partial \bar{p}}{\partial \bar{z}}\right) + Re^{-1}\frac{\partial^2(\bar{u}, \bar{w})}{\partial \bar{y}^2} \, , \tag{2}$$

$$\bar{u} = \bar{v} = \bar{w} = 0 \ \text{ at } \ \bar{y} = 0 \ \text{ (no slip)}, \tag{3}$$

$$\bar{u} \sim \bar{y} + A(\bar{x}, \bar{z}, \bar{t}) \ \ \bar{w} \to 0 \quad \text{as} \ \ \bar{y} \to \infty \ \ \text{(unknown displacement)}, \tag{4}$$

$$\bar{p}(\bar{x}, \bar{z}, \bar{t}) = -\frac{1}{2\pi}\int_{-\infty}^{\infty}\int_{-\infty}^{\infty} \frac{\partial^2 A/\partial \chi^2(\chi, \phi, T)d\chi d\phi}{[(\bar{x} - \chi)^2 + (\bar{z} - \phi)^2]^{1/2}} \ \ \text{(interaction law)}. \tag{5}$$

Here (5) applies for subsonic flow. Two alternatives to the above are Direct Numerical Simulations and IBL/related versions at finite *Re*. Both require numerical treatments. In general, the former is hindered by grid-resolution difficulties, among others. IBL and similar methods, which are zonal treatments involving sensible interpretations of (1)-(5) at finite *Re*, have been developed a little for unsteady flows (Smith *et al.* 1984, our Fig. 1, Peridier *et al.* 1991). These link with, and incidentally show the ellipticity implicit in, the parabolized stability equations (Bertolotti *et al.* 1992, Dr. M.R. Malik 1990's) developed successfully recently.

For strongly nonlinear amplitudes, the unsteady IBL system (1)-(5) yields localized finite-time breakups (Smith, 1988). These breakups have, in 2D, $\bar{x} - \bar{x}_s = c(\bar{t} - \bar{t}_s) + (\bar{t}_s - \bar{t})^N \xi$,

$$\frac{\partial \bar{p}}{\partial \bar{x}} \sim (\bar{t}_s - \bar{t})^{-1} p_1'(\xi), \ \ \bar{u} \to u_0(\bar{y}) \tag{6}$$

near the breakup position $\bar{x}_s$ and time $\bar{t}_s$. The local profile u_0 is smooth, $u_0 = c$ at the inflection point, ξ is 0(1), and the phase speed c is 0(1). The power $N = 3/2$ is the most likely. Approaching the breakup an inviscid Burgers equation

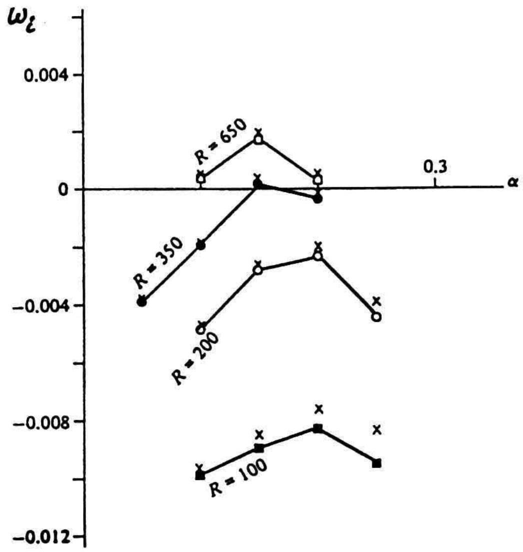

Figure 1: Comparison between IBL-related results (×) and Orr-Sommerfeld results for linear growth rates in Blasius flow, at subcritical and supercritical Reynolds numbers $R \sim Re^{1/2}$, from Smith *et al.* (1984).

governs $p_1(\xi)$, from integration in $\bar{y}$, provided the integral constraint (8) below on u_0 is satisfied. This gives $p_1(\xi)$, with $|p_1| \propto |\xi|^{1/3}$ at large $|\xi|$, so that

$$\bar{p} - p_0 \propto |\bar{x} - \bar{x}_s|^{1/3} \quad \text{as } \bar{x} \to \bar{x}_s \pm \tag{7}$$

where $p_0 \equiv \bar{p}(\bar{x}_s)$ is constant. Hence a singularity in pressure gradient is predicted at the breakup time $\bar{t} = \bar{t}_s$, as well as increasingly large wall-shear responses. IBL computations support (6), (7) as do some direct simulations, whereas experimental comparisons are described just below. The breakup applies to most unsteady interactive flows. Detailed quantitative comparisons between computations and theory in (6), (7) by Peridier *et al.* (1991) show good agreement.

New physical effects then come into play as normal pressure gradients become significant on shorter length scales. An appropriate computational approach in principle then is in Smith *et al.* (1984), Smith (1991). The new faster stage is discussed by Hoyle *et al.* (1991), He *et al.* (1996) where an extended KdV equation holds for the pressure, subject to matching with (6), (7). Beyond that, in still faster time scales a strong vortex formation takes place (Bowles *et al.*, 1996). This is associated with initiation and eruption of a vortex. Intuition suggests that this breakup process, repeated, is connected with intermittency. Smith and Bowles (1992) compare (see our Fig. 2) the breakup criterion (Smith,

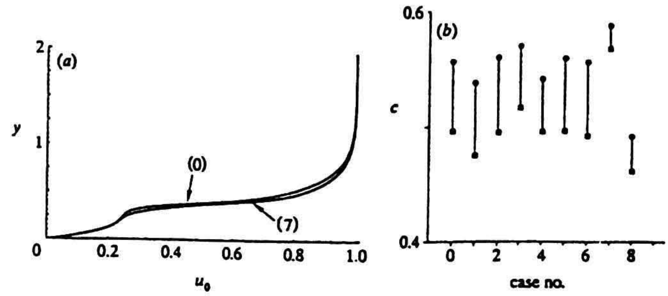

Figure 2: Comparisons between theory (Smith & Bowles, 1992) and experiment (Nishioka *et al.*, 1979), concerning the nonlinear criterion (8) and the first transitional spike. All the cases (0)-(8) studied are close to the two representative cases (0), (7) for the local experimental profile shown in (a). In (b), effectively the circles denote theoretical results and the squares experimental results. Note that the complete range of possible c values is between 0 and 1, and that the variation with case number in (b) indicates sensitivity with respect to the velocity-profile measurement.

1988) for (6), (7), namely

$$\int_0^\infty [u_0(\bar{y}) - c]^{-2} d\bar{y} = 0 \, , \tag{8}$$

with Nishioka *et al.*'s (1979) experiments concerning *the first spike*. The agreement is relatively close, given that *Re* is subcritical in the experiments.

There are many related or follow-on aspects. First, high-frequency theory applied to (1)-(5) yields an alternative view of spikes, associated more with still larger disturbances as discussed in item 3(e) below. In the same regime Kachanov *et al.* (1993) compare 2D nonlinear theory and experiments showing other apparent spikes, finding good agreement as shown in Fig. 3(a); while at suitably reduced amplitudes upper-branch features and critical layers tend to arise further downstream of the lower-branch regime (1)-(5). Second there is recent work by Vickers & Smith (1994) on break-up of separating flows; see also Savenkov (1993). Next, Hoyle & Smith (1994) consider the extension of (6)-(8) to 3D, where (8) again applies and

$$\bar{z} - \bar{z}_s \sim (\bar{t}_s - \bar{t})^{5/4} \tag{9}$$

gives a crucial spanwise scale. Likewise in 3D, Smith & Walton (1989), Stewart & Smith (1992) and Smith & Bowles (1992) imply that vortex/wave interactions based on (1)-(5) for example can act at low input amplitudes as precursors to the strong-amplitude finite-time break-up above. The latter two yield good agreement with boundary-layer and channel flow experiments (Figs 3b,c), in addition to that above. Other vortex/wave interactions are studied in the series by Hall & Smith (1988, 1989, 1990, 1991), with related works by Benney & Chow (1989), Wu (1993), Churilov & Shukhman (1987, 1988), Walton & Smith (1992), Timoshin & Smith (1995), Walton, Bowles & Smith (1994), Smith, Brown &

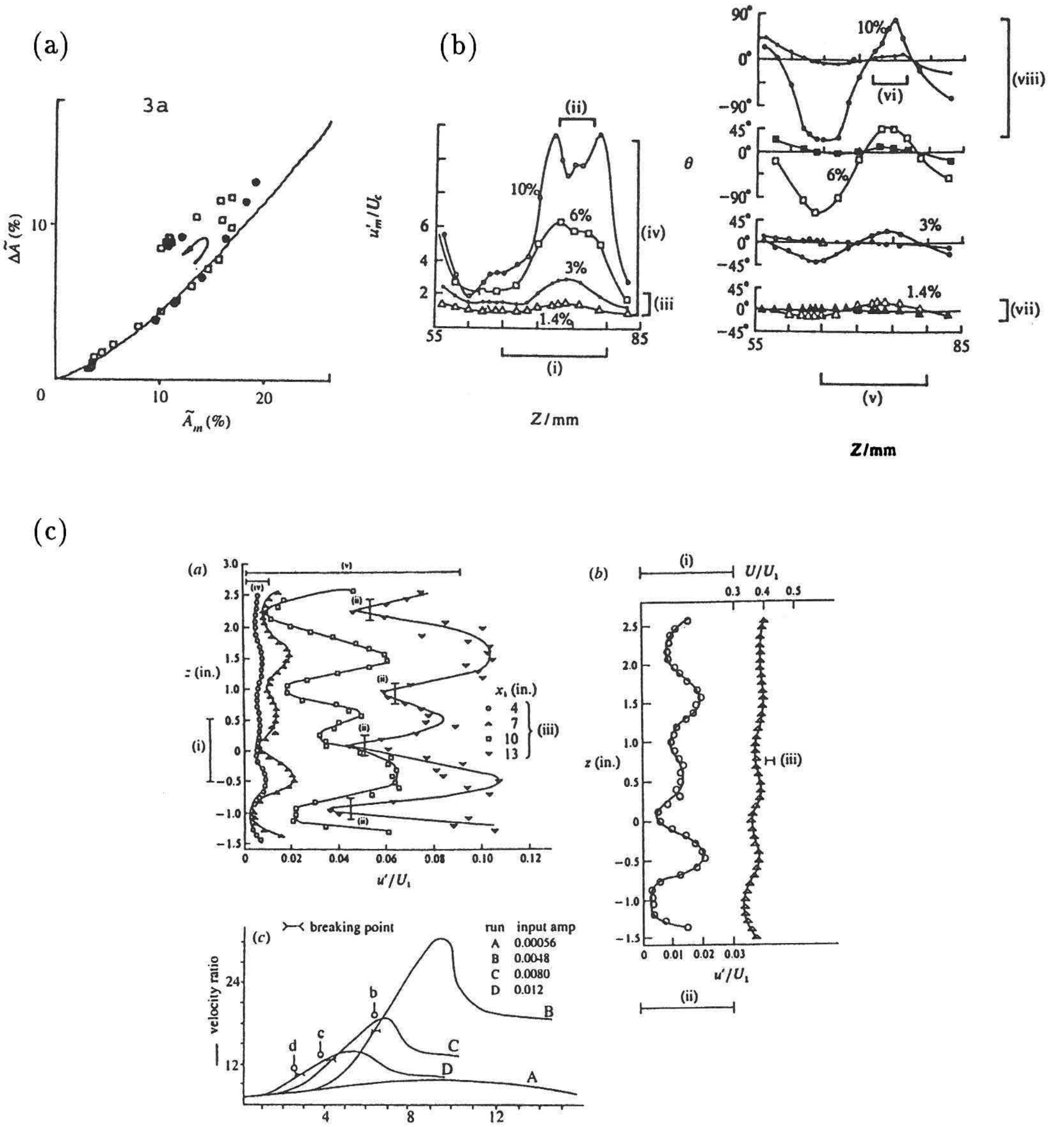

Figure 3: Further comparisons with experiments. (a) From Kachanov *et al.* (1993), in mostly quasi-2D transition. (b) From Smith & Bowles (1992), in the channel-flow 3D transition of Nishioka *et al.* (1979). Theoretical results are shown as bars (i) - (viii). (c) From Stewart & Smith (1992), in the boundary-layer 3D transition of Klebanoff & Tidstrom (1959). Theoretical predictions are indicated by bars (i) - (v) in the left-hand diagram, (i) - (iii) in the middle, and b,c,d (compared with experimental breaking points) in the right-hand diagram.

Brown (1993), in various weakly or strongly nonlinear settings with TS or inflectional disturbances. Hall & Smith (1988-1991) in particular emphasize the ability of vortex/wave interactions to provoke strongly nonlinear effects even for quite tiny 3D input disturbances. Vortex effects are clearly very powerful, both theoretically and in practice. Finally here, further work following on directly from (6)-(8) is mentioned later.

The transitional spot (item 3)

For free spots (cf. forced spots arising in item 2) the Euler stage has, throughout the boundary layer,

$$\overline{u}_x + \overline{v}_y + \overline{w}_z = 0\ , \tag{10}$$

$$(\partial_t + \underline{\bar{u}}.\underline{\nabla})\underline{\bar{u}} = -\underline{\nabla}\bar{p}. \tag{11}$$

The coordinates, with an origin shift, are scaled on the thickness $0(Re^{-1/2})$ and similarly for t, while

$$(\overline{u},\overline{v},\overline{w},\overline{p}) \to (u_B(y),0,w_B(y),0) \quad \text{as} \quad x^2+z^2 \to \infty, \tag{12}$$

$$(\overline{u},\overline{v},\overline{w},\overline{p}) \to (u_e,0,w_e,0) \quad \text{as}\, y \to \infty, \tag{13}$$

$$\overline{v} = 0 \quad \text{at} \quad y = 0, \tag{14}$$

with the undisturbed profile $u_B(y)$ holding far from the initial disturbance. For the present $u_e \equiv 1$, $w_e = w_B(y) \equiv 0$, but compare (d) below. The profile $u_B(y)$ is monotonic, inflexion-free, and $u_B(\infty) = 1$, $u'_B(0) = \lambda_B > 0$, and the initial disturbance itself has $(\overline{u},\overline{v},\overline{w},\overline{p})$ prescribed for all x,y,z at $t = 0$. The problem (10)-(14) is a computational one usually.

Smith *et al.* (1994) consider properties at large times, especially far downstream. Two major scales arise in the plan-view at distances $0(t^{1/2})$ and $0(t)$. See Fig. 4. In the $0(t^{1/2})$ zone, the solution takes on a three-layer form, the 'lowest' layer having

$$(\overline{u},\overline{v},\overline{w},\overline{p}) \sim \left[t^{-1}U,\ t^{-3/2}V,\ t^{-1/2}W,\ t^{-1}P\right],\ y = t^{-1/2}\overline{Y}\ , \tag{15}$$

and similarly for the 'middle' and 'uppermost' layers. The unknown surface pressure $P(\overline{X},\overline{Z})$ and negative displacement $A(\overline{X},\overline{Z})$ depend on $(\overline{X},\overline{Z})$ defined by

$$(x,z) = t^{1/2}(\overline{X},\overline{Z}). \tag{16}$$

From (10)-(14) a nonlinear similarity inviscid-boundary-layer-like system then holds. (a) - (c) below are concerned with the spot "trailing edge", where $(\overline{X},\overline{Z})$ are large, between the $0(t^{1/2})$ and $0(t)$ zones, the latter being discussed in (d), (e).

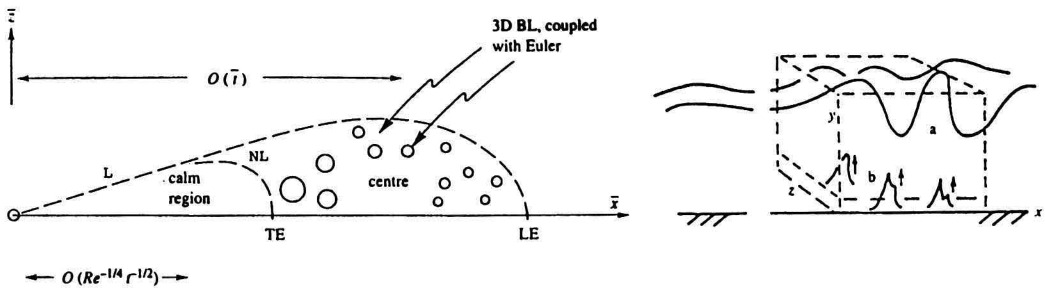

Figure 4: (a) Plan view of the theoretical spot structure in item 3, with symmetry about the $\bar{x}$-axis. In item 3(a-c) $Re^{-1/2} << \bar{t} << 1$, whereas when time $\bar{t}$ becomes 0(1), in item 3(d,e), coupling occurs between the global (3DBL) and local (Euler, see (b)) properties as indicated. $\mathcal{L}, \mathcal{NL}$ denote linear and nonlinear regions in turn, the former envisaged as bounding the calm region observed in experiments, while LE,TE denote the leading and trailing edges respectively. (b) The local 3D Euler structure a and subsequent sublayer eruptions b, leading to spots within spots: see item 2, item 3(e).

(a) *Amplitude level I*

At comparatively large distances $\overline{X} >> 1$ downstream, in the edge layer near $\overline{Z} \approx \mu\overline{X}$ (Fig. 4),

$$P = \overline{X}^{2/3}(Ep_0 + c.c.) + ... + \overline{X}^{-2/3}p_m + ... , \tag{17}$$

where $\mu = 8^{-1/2}$, $\overline{Z} - \mu\overline{X} = \overline{X}^{-1/3}\eta$, and the dominant fluctuating part (subscript zero) has $E = \exp\left[i(b_1\overline{X}^2 + \lambda\overline{X}^{2/3}\eta)\right], b_1 = 3^{3/2}/16$, $\lambda = (3/8)^{1/2}$, $\eta \sim 1$. The subscript m refers to the real mean-flow, and c.c. denotes the complex conjugate. The nonlinear interaction is dominated by the fluctuations $E^{\pm 1}$ and the mean-flow correction E^0,due physically to the relative slowness of the mean-flow variations; similarly in (b).

The governing equations (Smith *et al.*, 1994) stem from the outer interaction law and the relation $p_m \propto -|p_0|^2$ due to the mean components of momentum coupled with modulation by the mean-flow (vortex) correction. Sample solutions are presented in the last reference.

(b) *Amplitude level II*

Significant changes occur first when the amplitudes increase slightly and $\overline{Z} - \mu\overline{X} = \hat{\eta}$ becomes 0(1). Now

$$P = \overline{X}^{3/4}(\widehat{E}\widehat{p}_0 + c.c.) + ... + \overline{X}^{-1/2}\widehat{p}_m + ... \tag{18}$$

The fluctuation with unknown $\hat{f}(\hat{\eta})$, because of enhanced phase variations, is $\hat{E} = \exp\left[i(b_1\overline{X}^2 + \lambda\overline{X}\hat{\eta} + \overline{X}^{1/2}\hat{f}(\hat{\eta}))\right]$. New contributions come from extra momentum in the mean-flow, preserving the dominance of the long/short interaction between fluctuations and mean flow. Solutions are presented by Dodia *et al.* (1995). For enhanced amplitudes II there is a diminution of the mean-flow effect produced by the external motion. A new stage occurs when the whole trailing-edge region becomes affected by strong nonlinearity, as $\overline{Z} - \mu\overline{X}$ rises to $0(\overline{X})$. Then the mean-flow correction becomes comparable with the basic mean flow.

(c) *Amplitude level III affecting the entire trailing edge*

Here the amplitude of fluctuations and mean-flow parts is raised to $0(\overline{X})$, in U, W, with corresponding increases in V, P (Fig. 4). The interactions become *strongly nonlinear* and higher harmonic fluctuations are significant. In polars r, θ, where $(\overline{X}, \overline{Z}) = r(\cos\theta, \sin\theta), \theta$ is $0(1)$, with r being large, the flowfield solution has

$$\overline{U} = r(\overline{U}_m + \overline{U}_f) + \ldots, \quad \overline{W} = r(\overline{W}_m + \overline{W}_f) + \ldots, \quad P = r^2\overline{P}_f + (\overline{P}_m + P_f) + \ldots, \tag{19}$$

where $\overline{U}, \overline{W}$ are the r-, θ-velocities. The subscript f refers to fluctuations, having zero mean. The *total* mean flow, e.g. $\overline{U}_m$, is unknown now but varies slowly, being dependent on $\overline{Y}, \theta$, whereas unknown fluctuations, e.g. $\overline{U}_f$, also depend on the rapid variable $F \equiv b(\theta)r^2$. Smith *et al.* (1994) show that a closed nonlinear system is produced controlling the dominant fluctuations, the total mean flow, and the phase $b(\theta)$.

(d) *The spot centre*

Here, at larger distances $x \sim t$ downstream, the full Euler equations (10), (11) re-apply. The three-layer structure collapses into one and the x, z scale falls to $0(1)$ for fluctuations. (c) points to strong nonlinearity persisting here. The unsteady $3D$ Euler system holding implies a large numerical task. But also there is interplay between those fluctuations and the slow total mean flow. So extra length scales operate, x, z of $0(t)$ in addition to $0(1)$, associated with slender-flow equations for the mean, and they play an equally important role, linking the main short- and long-scale behaviour similarly to (c).

Moreover, as the spot continues downstream, to x, z of order $Re^{1/2}$ i.e. global distances of $0(1)$, the interacting short- and long-length scales become $0(Re^{-1/2})$ and $0(1)$ respectively, in the global coordinates $\bar{x}$, $\bar{z}$, with the normal coordinate staying $0(Re^{-1/2})$. These scalings are physically sensible. Viscous forces now affect the mean-flow through the 3D boundary-layer equations

$$\bar{u}_{\bar{x}} + \bar{v}_y + \bar{w}_{\bar{z}} = 0\,, \tag{20}$$

$$\bar{u}_{\bar{t}} + \bar{u}\bar{u}_{\bar{x}} + \bar{v}\bar{u}_y + \bar{w}\bar{u}_{\bar{z}} = \bar{s}_1 - \bar{p}_{\bar{x}} + \bar{u}_{yy} \,, \tag{21}$$

$$\bar{w}_{\bar{t}} + \bar{u}\bar{w}_{\bar{x}} + \bar{v}\bar{w}_y + \bar{w}\bar{w}_{\bar{z}} = \bar{s}_2 - \bar{p}_{\bar{z}} + \bar{w}_{yy} \,, \tag{22}$$

for the mean-flow $(\bar{u}, \bar{v}, \bar{w})(\bar{x}, y, \bar{z}, \bar{t})$, where $\bar{t} \equiv Re^{-1/2}t$ denotes global time. Here $\bar{p}(\bar{x}, \bar{z}, \bar{t})$ is the external-stream pressure, whereas $\bar{s}_1, \bar{s}_2$ are the unknown Reynolds-stress terms comprising nonlinear effects from the fluctuating velocity components governed by (10)-(14). The full interaction between (20)-(22) and (10)-(14) also involves the mean profile $\bar{u} = u_B$ in (13), which is now dependent on $\bar{x}, y, \bar{z}, \bar{t}$ and unknown, as is the corresponding nonzero $\bar{w} = w_B$ in general. It is intriguing that, according to the above argument, the flow properties on those two length scales remain fully interactive, with the viscous $3D$ boundary-layer system (20)-(22) and the inviscid $3D$ Euler system (10)-(14) being coupled together via the Reynolds stresses in (21), (22) and the profiles in (13). See Smith *et al.*'s (1994) Fig. 4 and our Fig. 4.

(e) *Internal dynamics and viscous effects*

The major element missing so far in item 3 is viscosity, governing the finer-scale dynamics and the connection with larger scales, apart from the global-scale effect in (20)-(22) etc.. Although our concern in the majority of item 3 is with global features, internal features are considered briefly in Smith (1995), more details and description being given in item 2 and in references cited.

Further comments (item 4)

There is still much to be explained. Further work is needed to understand the impact of the eruptive sublayer (item 2) on the larger-scale evolution in item 3, and the generation of faster time and length scales.

Yet the global spot theory tentatively is in line with the experimental findings summarized in item 1 in a qualitative or quantitative sense. Bowles & Smith (1995) point to important short-scaled effects combining with nonlinearity above to give a theoretical spread angle (Fig. 5) of approximately 11°, close to the experimental observations, for zero pressure gradient. On compressibility effects, Clark *et al.*'s (1994) results demonstrate experimental agreement with the theory over a range of Mach numbers (Fig. 6). On internal features quantitative agreement with computations and experiments has been noted in item 2 and is shown in Figs 2 and 3; in particular the breaking point in Fig. 3(b) signals the onset of turbulent spots in the forced flow there, linking with the free type of spot considered in item 3. Comparisons of the integral criterion (8) with direct simulations have been attempted, in addition to those with experiments in Fig. 2 which we repeat are at *subcritical* Reynolds numbers, indicating wide application of the theory (see also Fig. 1).

The same criterion (8) applies to the onset of transition in 3D over surface roughnesses and similar flows (FTS with D.J. Savin). Other 3D theory is developing, e.g. vortex/wave interactions. The repercussions for 3D computation

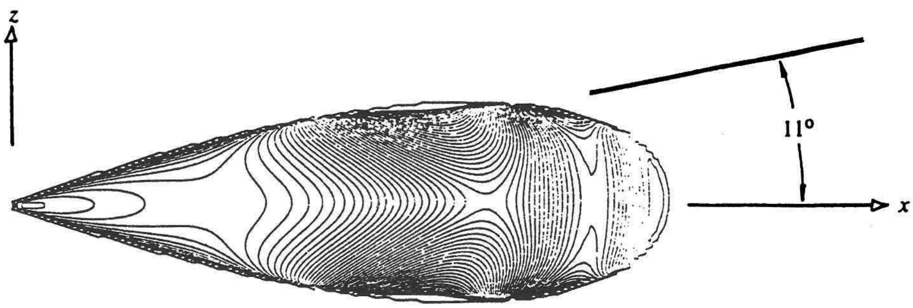

Figure 5: Theoretical spot solution from Bowles & Smith (1995) incorporating short-scale effects, and comparison with the typical 11° spread angle found experimentally.

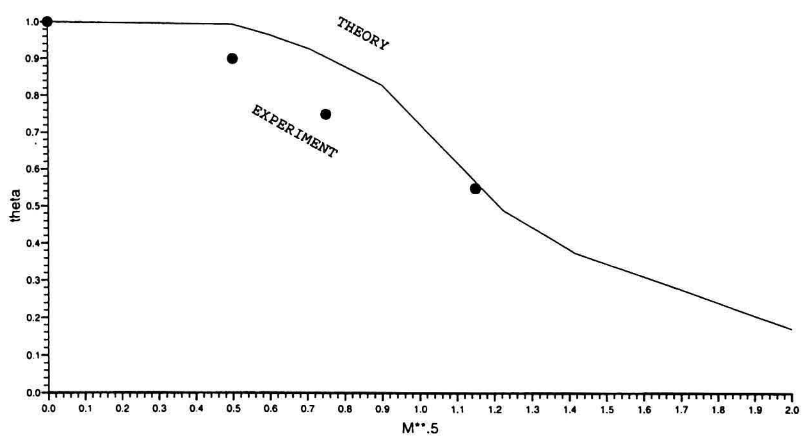

Figure 6: Spot spreading angle vs. Mach number, for compressible boundary layers, from Clark *et al.*'s experiments (1994) and theory by Dr. R.G.A. Bowles with FTS (1995), following on from Bowles & Smith (1995).

are fairly clear, given the resolution difficulties of direct simulations at large Re. Item 2 implies that an IBL-type system is needed but supplemented by Euler terms, because of normal pressure gradient effects (item 2, end) along with item 3 and Bowles & Smith's (1995) results. The composite system of Smith *et al.* (1984), Smith (1991b) has these in unsteady 2D flows (Fig. 1), while 3D steady computations (Smith 1991a) indicate accuracy and efficiency. Work is in progress on the 3D unsteady extension but it needs more attention.

References

Benney, D.J. & Chow, C. 1989 – *Studies in Appl. Math.* **80**, 37-62.

Bertolotti, F.P., Herbert, Th. & Spalart, P.R. 1992 – Linear and nonlinear stability of the Blasius Boundary layer, *J. Fluid Mech.* **242**, 442-474.

Bowles, R.G.A. & Smith, F.T. 1995 – Short-scale effects on model boundary-layer spots, *J. Fluid Mech.* **295**, 395-407.

Bowles, R.I., Smith, F.T. & Walker, J.D.A. 1996 – to be submitted.

Churilov, S.M. & Shukman, I.G. 1987 – Nonlinear stability of a stratified shear flow: a viscous critical layer, *J. Fluid Mech.* **180**, 1-20.

Churilov, S.M. & Shukman, I.G. 1988 – Nonlinear stability of a stratified shear flow in the regime with an unsteady critical layer, *J. Fluid Mech.* **194**, 187-216.

Clark, J.P., Jones, T.V. & LeGraff, J.E. 1994 – On the propagation of naturally-occurring turbulent spots, *J. Eng. Math.* **28**, 1-19.

Dodia, B.T., Bowles, R.G.A. & Smith, F.T. 1995 – Tto appear in *J. Eng. Math.*.

Hall, P. & Smith, F.T. 1988 – The nonlinear interaction of Tollmien-Schlichting waves and Taylor-Görtler vortices in curved channel flows, *Proc. Roy. Soc.* **A417**, 255-282.

Hall, P. & Smith, F.T. 1989 – Nonlinear Tollmien-Schlichting/vortex interaction in boundary layers, *Europ. J. Mechs* **B8**, 179-205.

Hall, P. & Smith, F.T. 1990 – Near-planar TS waves and longitudinal vortices in channel flow: nonlinear interaction and focussing. In Instability and Transition II, eds. Hussaini, M.Y. and Voigt, R.G., Springer.

Hall, P. & Smith, F.T. 1991 – On strongly nonlinear vortex-wave interactions in boundary layer transition, *J. Fluid Mech.* **227**, 641-666; also 1989, Institute for Computer Appl. in Sc. & Eng., Rept. 89-92.

He, J., Walker, J.D.A., Bowles, R.I. & Smith, F.T. 1996 – To be submitted.

Henningson, D.S., Johansson, A.V. & Alfredson, P.H. 1994 – Turbulent spots in channel flows, *J. Eng. Maths.* **28**, 21-42.

Hoyle, J.M., Smith, F.T. & Walker, J.D.A. 1991 – On sublayer eruption and vortex formation, *Comp. Phys. Comms* **65**, 151-157; also Hoyle, J.M., 1992, Ph.D. Thesis, London Univ., London.

Hoyle, J.M. & Smith, F.T. 1994 – On finite-time break-up in three-dimensional unsteady interacting boundary layers, *Proc. Roy. Soc.* **A 447**, 467-492.

Kachanov, Y.S., Ryzhov, O.S. & Smith, F.T. 1993 – Formation of solitons in transitional boundary layers: theory and experiment, *J. Fluid Mech.* **251**, 273-297.

Klebanoff, P.S. & Tidstrom, K.D. 1959 – The evolution of amplified waves leading to transition in a boundary layer with zero pressure gradient, Tech. Notes Nat. Aero. Space Admin., Wash., D-195 (see in 1963, Stuart, J.T., Ch. IX of Laminar Boundary Layers, ed. Rosenhead, L.)

Nishioka, M., Asai, M. & Iida, S. 1979 – An experimental investigation of the secondary instability, in Laminar-Turbulent Transition, Springer-Verlag.

Peridier, V.J., Smith, F.T. & Walker, J.D.A. 1991 – Vortex -induced boundary-layer separation. Part 2. Unsteady interacting boundary layer theory, *J. Fluid Mech.* **232**, 132-165.

Savenkov, I.V. 1993 – Wave packets, resonant interactions and soliton formation in inlet pipe flow, *J. Fluid Mech.* **252**, 1-30.

Seifert, A., Zilberman, M. & Wygnanski, I. 1994 – On the simultaneous measurements of two velocity components in the turbulent spot, *J. Eng. Maths* **28**, 43-54.

Shaikh, F.N. & Gaster, M. 1994 – The non-linear evolution of modulated waves in a boundary layer, *J. Eng. Math.* **28**, 55-71.

Smith, C.R., Walker, J.D.A., Haidari, A.H. & Sobrun, U. 1991 – On the dynamics of near-wall turbulence, *Phil. Trans. R. Soc.* **A336**, 131-175.

Smith, F.T., Papageorgiou, D.T. & Elliott, J.W. 1984 – An alternative approach to linear and nonlinear stability calculations at finite Reynolds numbers, *J. Fluid Mech.* **146**, 313-330.

Smith, F.T. 1988 – Finite-time break-up can occur in any unsteady interacting boundary layer, *Mathematika* **35**, 256-273.

Smith, F.T. & Walton, A.G. 1989 – Nonlinear interaction of near-planar TS waves and longitudinal vortices in boundary-layer transition, *Mathematika* **36**, 262-289.

Smith, F.T. 1991a, Steady and unsteady 3-D interactive boundary layers, *Comp. & Fluids* **20**, 243-168. (Also given as a presentation at the R.T. Davis Memorial Symp., Cincinnati, U.S.A. (1987).)

Smith, F.T. 1991b – Composite, Navier-Stokes and Euler unsteady-flow computations in boundary layers, Utd. Tech. Res. Cent. Rept. UTRC91-2, Hartford, CT; Composite, Navier-Stokes and Euler unsteady-flow computations in boundary layers, *J. Eng. Maths*, in press (1996).

Smith, F.T. & Bowles, R.I. 1992 – Transition theory and experimental comparisons on (I) amplification into streets and (II) a strongly nonlinear break-up criterion, *Proc. Roy. Soc.* **A439**, 163-175.

Smith, F.T., Dodia, B.T. & Bowles, R.G.A. 1994 – On global and internal dynamics of spots: a theoretical approach, *J. Eng. Math.* **28**, 73-91.

Smith, F.T., Brown, P.G. & Brown, S.N. 1993 – Initiation of three-dimensional nonlinear transition paths from an inflexional profile, *Europ. J. Mech.* **12**, 447-473.

Smith, F.T. 1995 – On spikes and spots: Strongly nonlinear theory and experimental comparisons, *Phil. Trans. Roy. Soc.* **A352**, 405-424.

Stewart, P.A. & Smith, F.T. 1992 – Three-dimensional nonlinear blow-up from a nearly planar initial disturbance, in boundary-layer transition: theory and experimental comparisons, *J. Fluid Mech.* **244**, 79-100.

Timoshin, S.N. & Smith, F.T. 1995 – Vortex/inflectional-wave interactions with weakly three-dimensional input. Parts I, II, *J. Fluid Mech.*, submitted.

Vickers, I.P. & Smith, F.T. 1994 – Theory and computations for breakup of unsteady subsonic or supersonic separating flows, *J. Fluid Mech.* **268**, 147-173.

Walton, A.G. & Smith, F.T. 1992 – Properties of strongly nonlinear vortex/Tollmien-Schlichting waves interactions, *J. Fluid Mech.* **244**, 649-676.

Walton, A.G., Bowles, R.I. & Smith, F.T. 1994 – Vortex/wave interaction in separating flows, *Europ. J. Mechs.* **B13**, 629-655.

Wu, X. 1993, Nonlinear temporal-spatial modulation of near-planar Rayleigh waves in shear flows: formation of streamwise vortices, *J. Fluid Mech.* **256**, 685-719.

Author's address

University College London
Department of Mathematics
Gower Street, London WC1E 6BT, UK